Environmental Science
Processes & Impacts

Accepted Manuscript

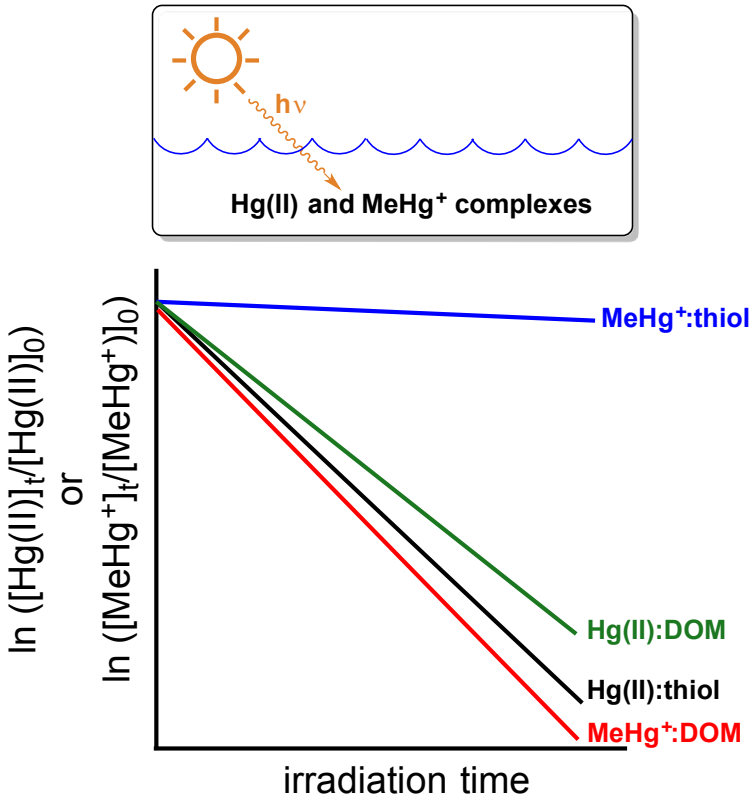

Summary Statement: Photochemical experiments demonstrate potential mechanistic differences between the photodemethylation of methylmercury and photoreduction of mercury(II) attached to dissolved organic matter

Mercury contamination of aquatic and terrestrial food chains is a serious problem impacting human and ecological health. This work investigates the mechanisms of photoreduction of Hg(II) and photodemethylation of methylmercury highlighting the key role of dissolved organic matter. Both of these processes are of primary importance in the fate and transport of mercury in the global environment. Understanding the mechanism and kinetics of photodemethylation in the presence of dissolved organic matter is a key component in modeling the persistence of methylmercury in aquatic systems; photoreduction is an important process for transferring mercury from aquatic systems to the atmosphere.

Photoreduction of Hg(II) and photodemethylation of methylmercury: The key role of thiol sites on dissolved organic matter

Jeffrey D. Jeremiason[1*], Joshua C. Portner[1], George R. Aiken[3], Amber J. Hiranaka, Michelle T. Dvorak, Khuyen T. Tran, and Douglas E. Latch[2]*

[1]Gustavus Adolphus College, St Peter, MN.

[2]Seattle University, Seattle, WA.

[3]US Geological Survey, Boulder, CO.

* corresponding authors: jjeremia@gustavus.edu, latchd@seattleu.edu

Abstract

This study examined the kinetics of photoreduction of Hg(II) and photodemethylation of methylmercury ($MeHg^+$) attached to, or in the presence of, dissolved organic matter (DOM). Both Hg(II) and $MeHg^+$ are principally bound to reduced sulfur groups associated with DOM in many freshwater systems. We propose that a direct photolysis mechanism is plausible for reduction of Hg(II) bound to reduced sulfur groups on DOM while an indirect mechanism is supported for photodemethylation of $MeHg^+$ bound to DOM. UV spectra of Hg(II) and $MeHg^+$ bound to thiol containing molecules demonstrate that the Hg(II)-S bond is capable of absorbing UV-light in the solar spectrum to a much greater extent than $MeHg^+$-S bonds. Experiments with chemically distinct DOM isolates suggest that concentration of DOM matters little in the photochemistry if there are enough reduced S sites present to strongly bind $MeHg^+$ and Hg(II); DOM concentration does not play a prominent role in photodemethylation other than to screen light, which was demonstrated in a field experiment in the highly colored St. Louis River where photodemethylation was not observed at depths ≥ 10 cm. Experiments with thiol ligands yielded slower photodegradation rates for $MeHg^+$ than in experiments with DOM and thiols; rates in the presence of DOM alone were the fastest supporting an intra-DOM mechanism. Hg(II) photoreduction rates, however, were similar in experiments with only DOM, thiols plus DOM, or only thiols suggesting a direct photolysis mechanism. Quenching experiments also support the existence of an intra-DOM photodemethylation mechanism for $MeHg^+$. Utilizing the difference in photodemethylation rates measured for $MeHg^+$ attached to DOM or thiol ligands, the binding constant for $MeHg^+$ attached to thiol groups on DOM was estimated to be $10^{16.7}$.

Introduction

Dissolved organic matter (DOM) and photochemical processes are important controls for mercury cycling in aquatic systems. Photochemical processes have been demonstrated to oxidize Hg^o, reduce Hg(II), and demethylate methylmercury ($MeHg^+$); however, the reaction pathways are not clearly understood. Reduced sulfur groups in DOM are strong ligands for Hg(II) and $MeHg^+$ and control their speciation in most freshwater systems [1, 2]. DOM attenuates incoming light, but is also a major source of an array of photochemically produced reactive intermediates (PPRIs) in sunlit waters including singlet oxygen ($^1O_2$), hydroxyl radical (·OH) and other radical species, and triplet excited state DOM ($^3DOM^*$) [3, 4].

Several studies have demonstrated that Hg(II) can be photochemically reduced in natural waters. This photoreduction has been shown in field studies[5-7] in which the diurnal variations in Hg speciation and light intensity were monitored over time, and in laboratory-based studies. Photoreduction of Hg(II) is influenced by binding to DOM and PPRIs, and photolysis of mercury thiol species have been implicated in this process [8].

The photodemethylation of $MeHg^+$ has also been widely reported, and many recent studies have proposed mechanisms [9-12]. $MeHg^+$ is demethylated in the presence of both photosynthetically active radiation (PAR 400-700 nm) and ultraviolet radiation (UV), but studies have produced wavelength-specific rate constants showing that UVB radiation (280-320 nm) degrades $MeHg^+$ more rapidly than UVA radiation (320-400 nm) or PAR [1, 3, 13]. Complexation by DOM and thiol-based ligands also affects $MeHg^+$ photodemethylation rates [10, 12], but the degree to which the rate changes varies with different studies [10-12]. Although attempts have been made to gain insight into multiple variables affecting photodemethylation, many reaction pathways are possible making the relative importance of various factors dependent on experimental conditions.

Two basic mechanisms have been considered for both Hg(II) photoreduction and photodemethylation of $MeHg^+$ in the presence of DOM: (1) direct absorption of light by the C-Hg bond of $MeHg^+$, the Hg-S bond of DOM bound Hg, or by the DOM with energy transfer to an Hg bond; or (2) an indirect mechanism involving PPRIs. Direct absorption of light by DOM and energy transfer leading to demethylation has been proposed for $MeHg^+$ [11], and for inorganic Hg(II) reduction. Photodemethylation of $MeHg^+$ can be mediated by PPRIs as demonstrated in several lab studies. One recent study reported that $^1O_2$ produced by DOM after absorbing light leads to breakage of the methylmercury C-Hg bond that has been weakened due to Hg binding with a reduced S group on the DOM [3]. Binding to a reduced S group pulls electrons toward S increasing the electronegativity of C, reducing the C-Hg bond enthalpy leading to susceptibility to electrophilic attack by $^1O_2$. While this area of research into the specific mechanism of photodemethylation is in its relative infancy, several studies suggest that the MeHg-S bond is critical to its photoreactivity [1, 3, 12].

A recent study by Fernández-Gómez et al. [3] using different natural water samples with a wide range in DOM and iron concentrations, pH, and DOM aromaticities showed that wavelength-specific $MeHg^+$ degradation rates decreased with increasing absorption coefficients of the water samples. Once accounting for light attenuation caused by the absorbing components in the water samples, however, it was revealed that all of the samples converged to a give a common photodemethylation rate constant at a given irradiation wavelength. This finding is somewhat counterintuitive, as it suggests that so long as there exist reduced S sites for binding, the exact nature and chemical characteristics of the DOM is unimportant to the rate of $MeHg^+$ photodemethylation. Furthermore, Fernández-Gómez et al. [3] conducted experiments spanning a range of $MeHg^+$:DOM ratios, whereby at high ratios $MeHg^+$ is forced to bind to O and N functional groups due to saturation of the more favorable reduced S binding sites. Given that degradation rates decreased as $MeHg^+$:DOM ratios increased (and binding to O and N ligands occurs), their results corroborate the idea that binding of $MeHg^+$ to reduced S is key to photodemethylation. A final significant finding arising from their

work is that degradation rates sharply decrease as irradiation wavelength increases from UVB to UVA to PAR regions of the spectrum.

In this paper we present the results of field and laboratory experiments designed to elucidate the mechanistic roles that DOM plays in Hg(II) photoreduction and $MeHg^+$ photodemethylation processes. Our overall objective is to demonstrate similarities and to highlight some potential key differences in the photochemistry of Hg(II) and $MeHg^+$ that occur when Hg is bound to DOM. When considered over a range of DOM concentrations, these differences in photochemistry could affect cycling and persistence of Hg(II) and $MeHg^+$ in sunlit surface waters. Additional experiments were performed with $MeHg^+$ to determine the wavelength dependence of the photodemethylation process and to demonstrate the key role of the inner filter effect caused by DOM in limiting photodemethylation to only very near-surface depths in the highly-colored St. Louis River (MN).

Methods

A. Laboratory Studies

DOM isolates and water sampling. For $MeHg^+$ experiments, a sufficient amount of DOM was obtained from two sites in the St. Louis River watershed (Manganika Lake and St. Louis River Mile 94) in June of 2012 by pumping 60 to 150 L of water through 0.2 µm capsule filters. The DOM was separated by XAD-8/XAD-4 resins into three fractions which included the hydrophobic organic acid (HPOA), the transphilic acid fraction, and a hydrophilic fraction [14]. The DOM used in the $MeHg^+$ photodemethylation experiments were the HPOA fraction from Manganika Lake, the filtered St. Louis River whole water, and commercially available fulvic acids (Suwannee River, SRFA; and Pony Lake, PLFA; International Humic Substances Society). Additional DOM isolates were used in the study of Hg(II) photoreduction. These isolates come from a wide variety of natural waters and descriptions of these sites are given in Table 1. Table 2 includes characterization data for the isolates. Humic and fulvic acids are also isolated from water samples using resin techniques. Humic acid is the fraction of resin eluate that is insoluble at pH 1. The soluble portion is defined as fulvic acid.

Laboratory photolysis experiments. Two types of photochemical apparatuses were used: (*i*) a Suntest XLS+ solar simulator equipped with a broadband Xe lamp and a special UV filter to closely mimic the solar spectrum and (*ii*) a Luzchem photoreactor with interchangeable UVA and UVB light sources. Experimental design was similar for the two light sources. The Suntest XLS+ was operated at an output of 765 Wm^{-2}, while the UVA (~55 Wm^{-2}) and UVB (~66 Wm^{-2}) lamps were not as intense. The broadband lamp emits wavelengths between 300 and 800 nm, while the UVA lamp has 95% of its output between 316 and 400 nm (2.19% is

between 281 and 351 nm (UVB) and 0.67% is UVC between 235 and 289 nm). The UVB lamp has 53.94% in the UVB range, 32.04% in the UVA range, and 3.13% in UVC.

In all photolysis experiments, pH buffered solutions containing DOM isolates and/or thiol ligands were spiked with Hg(II) or $MeHg^+$ (final concentration ~0.5 nM) and placed into quartz culture tubes (*d* = 1 cm, *V* = 10 mL) to be irradiated. For all results reported herein using DOM isolates, solution pH was set to 7.0 using a 10 mM phosphate buffer. Additional experiments at pH 6 and pH 8 (data not shown) show that Hg(II) photoreduction and $MeHg^+$ photodemethylation rates did not vary over this limited pH range. Samples were removed at specific time intervals and immediately preserved. Hg(II) samples were preserved with BrCl and $MeHg^+$ samples were preserved with HCl until analysis. Spike levels of Hg(II) and $MeHg^+$ were calculated to ensure that binding would be dominated by reduced S groups[2] in all experiments while also being relevant to ambient environmental concentrations (sub nM).

All Hg(II) photoreduction experiments were conducted using the Suntest solar simulator. Solutions of Hg(II) were prepared in 125-mL I Chem bottles using ultrapure Milli-Q water. Samples were sparged with He, N_2, or air for at least 10 minutes immediately prior to initiating the photochemical experiments to remove any Hg(0). The samples were then each individually bubbled with the sparge gas throughout the course of the photolysis experiments to remove Hg(0) formed in the reduction process. The identity of the sparge gas did not impact the measured photoreduction rate constants (data not shown). Relatively short time points were chosen in order to minimize the impact of photooxidation of the evolved Hg(0) on fitting the photoreduction data to a simple first-order kinetic model. Control experiments showed that Hg(II) was not lost to the walls of the quartz test tubes. To limit inner filter effects over the wavelength range where Hg(II):thiol complexes absorb (see below), photoreduction experiments with different DOM isolates were performed at DOM concentrations that gave A = 0.05 at 310 nm in a 1-cm cuvette. Concentrations of the various DOM isolates used in these Hg(II) photoreduction experiments are as follows: 6.9 mg L^{-1} 2BS HPOA, 11.8 mg L^{-1} 2BS TPIA, 2.7 mg L^{-1} Suw. R. HA, 4.9 mg L^{-1} Suw R. FA, 5.1 mg L^{-1} Sac. R. HPOA, 12.2 mg L^{-1} Sac. R. TPIA, 4.1 mg L^{-1} Coal Creek FA, 6.8 mg L^{-1} Ohio R. FA, 2.2 mg L^{-1} IHSS peat HA, and 12.8 mg L^{-1} L. Fryxell FA. Additional experiments were performed with select DOM isolates (F1 HPOA, SRFA, and PLFA) to determine how DOM concentration impacts Hg(II) photoreduction and $MeHg^+$ photodemethylation rates. The thiol ligands used in Hg(II) photoreduction experiments were: mercaptoacetic acid (MAA) and glutathione (GSH). Reported error ranges are calculated standard error values of the regressed slopes of the linearized kinetic time courses.

MeHg+ photolysis experiments were conducted using both of the photochemical apparatuses. In addition to assessing how broadband, UVA, and UVB irradiation impacted $MeHg^+$ photodemethylation, the impacts of altering the following parameters on photodemethylation rates were assessed: DOM concentration (5 – 30

mgL^{-1}), DOM type (terrestrial versus microbial origin), and thiol ligand. MAA and GSH were used as thiol compounds to model potential reduced S binding sites on DOM and to alter the distribution of $MeHg^+$ between DOM and the thiol compounds. Experiments were also performed in filtered St. Louis River water.

Non-photochemical singlet oxygen reaction and measurement of $^1O_2$ steady-state concentration. The importance of $^1O_2$ in the photodemethylation of $MeHg^+$ was studied utilizing the disproportionation of hydrogen peroxide by molybdate anion as a $^1O_2$ source. Furfuryl alcohol (FFA) was used to validate the method [15]. Experiments were performed in the dark in a 10- mL Erlenmeyer flask containing 1.0 nM $MeHg^+$, 1.0 mM MAA, 10 mM FFA, 5 mM MoO_4^{2-}, 20 mM phosphate buffer (pH 7.0), and 0.20 M H_2O_2. After H_2O_2 addition, aliquots were taken at time intervals of 0, 5, 10, 15, 20, 25, 30, and 45 minutes and pipetted into a solution of 500 mM NaN_3 to quench any remaining $^1O_2$. FFA concentration was monitored by high-performance liquid chromatograph (HPLC-UV; Hewlett Packard 1090). $MeHg^+$ was analyzed via an inductively coupled plasma mass spectrometer (ICP-MS) as described below. In order to determine steady-state concentration of $^1O_2$ in PLFA solutions, a photolysis experiment with FFA was also performed. A 10 mg L^{-1} solution of PLFA at pH 7.0 with added FFA (10 μM) was irradiated at 765 W m^{-2} in the Suntest solar simulator.

B. Analytical Methods

Aliquots of one mL to six mL were analyzed for Hg(II) and $MeHg^+$ content. $MeHg^+$ was analyzed after pH adjustment and ethylation with sodium tetraethylborate by an isotope dilution method [16] on an Agilent 7700 ICP-MS with sample introduction via a MERX-M system (Brooks Rand). Hg(II) was analyzed by a dual-amalgamation technique using cold vapor atomic fluorescence spectroscopy (Tekran 2500) following standard BrCl oxidation/$SnCl_2$ reduction.

UV-vis Spectroscopy. Spectra were obtained on a dual path Agilent Cary Series 100 UV-Vis Spectrophotometer using long-path length quartz absorption cells (10 cm). Stock solutions of $HgCl_2$ and MeHgCl preserved in HCl were used to make Hg solutions. Thiol stock solutions were made from ACS grade or higher MAA, GSH, L-cysteine, N-acetyl-L-cysteine, thiolactic acid, and benzomercaptan. Spectra were obtained from solutions of Hg(II), $MeHg^+$, individual thiols, and Hg species mixed with thiol ligand at various concentrations.

C. Field Study

A field campaign was carried out in the St. Louis River from August 7-9, 2013 at river mile 94 (lat/long = 47.16729, -92.77927). During the field sampling two sets of experiments were conducted on a single water sample. About 20 liters of St. Louis River water were collected and filtered (0.7 µm glass fiber filters) directly

into a 20-L polypropylene carboy late in the day on August 6. The filters were ashed at 450° C and the Teflon filter holders were soaked in 4 M HCl and thoroughly rinsed with Milli-Q water (>18 mΩ-cm) and dried before use. The filtered water was spiked to a concentration of approximately 15 ng L^{-1} of $MeHg^+$, although the absolute concentration was unknown due to uncertainty in the volume of water. The water was stored refrigerated and allowed to equilibrate overnight. In the morning, the water was distributed to 10 mL quartz bottles and several 500- or 1000-mL dark Teflon bottles. The dark Teflon bottles served as dark controls during the experiments. Wire was wrapped around the caps of the quartz tubes and they were attached to a wooden stake driven into the river bed. Deeper bottles (depths were 0, 10, 20, and 40 cm) had progressively longer wires to prevent shading from above. Stakes containing bottles at the depths stated above were removed at 1 h, 2 h, 4 h, 1 d, 2 d, and 3 d. At each photodemethylation time point, the samples were immediately placed in a cooler and acid preservative was added while in the shade.

Results and Discussion

UV-Vis spectra for Hg(II) and $MeHg^+$ thiol complexes

To elucidate potential photochemical mechanisms and demonstrate fundamental differences between Hg(II) and $MeHg^+$, UV spectra were obtained for Hg(II) and $MeHg^+$ bound to simple reduced thiol molecules. Figure 1 shows individual spectra obtained for Hg(II) and $MeHg^+$ (0.1 mM) complexed with MAA and GSH (each at 1.0 mM). The UV spectra for Hg(II), $MeHg^+$, and the thiol ligands when measured alone did not have any overlap with the solar spectrum. Upon mixing the ligands and Hg(II), the absorbance spectrum shifts to longer wavelengths, with a significant tail > 290 nm. These spectra reveal that the Hg(II):thiol complexes absorb much more strongly and at longer wavelengths than the corresponding $MeHg^+$:thiol complexes and the free Hg(II) and thiol species. Si and Ariya [17] found similar absorption shifts for Hg(II) and simple alkanethiols. In terms of potential photochemical consequences, the absorption tail at λ > 290 nm exhibited by the Hg(II):thiol complexes mean that these species are capable of absorbing sunlight (and simulated sunlight) and thus may be more susceptible to direct photodegradation (i.e. reduction initiated by energy gained in the light absorption process by the Hg(II):thiol chromophore rather than from other chromophores or exogenous PPRIs). The maximum overlap between the Hg(II):thiol complexes and the solar spectrum was found to be at ca. 310 nm. In contrast, the spectra of $MeHg^+$:thiol complexes do not significantly overlap with the solar spectrum. Due to the minimal overlap with the solar spectrum, photodemethylation of $MeHg^+$:thiol complexes are expected to proceed through indirect photochemical pathways (i.e. reaction with PPRIs or energy transfer from other chromophores within $MeHg^+$:DOM complexes).

The UV spectra gave similar molar absorptivity values (over the wavelength range 280 – 340 nm) for each of the Hg(II):thiol complexes regardless of the identity of the thiol, with the exception of MAA, which had a higher absorptivity than the others (as demonstrated compared to GSH in Figure 1). Because Hg(II)interactions with DOM are dominated by thiol sites within the DOM, similar absorptivities to the model complexes would be expected for Hg(II)-S sites within Hg(II):DOM complexes. Thus, it is reasonable to expect that the direct photoreduction kinetics of the Hg(II):DOM complexes should be similar to those of the Hg(II): thiol complexes in optically dilute solutions. Analogously, the $MeHg^+$:thiol complexes exhibited similar absorptivities over the same wavelength window described for the Hg(II):thiols, and $MeHg^+$-S sites within $MeHg^+$:DOM complexes would be expected to have similar absorptivities and undergo little to no direct photodemethylation.

Effects of DOM on Hg(II) photoreduction

The photoreduction rate of Hg(II) was monitored at different concentrations of added DOM. Figure 2 shows the Hg(II) photoreduction rate constants measured over a range of DOM concentrations. There was no relationship between photoreduction rate constants and F1 HPOA concentration over the range of 2 to 20 mg L^{-1} DOM, with all concentrations giving similar results. Over this concentration range, all of the Hg(II) is expected to be bound to the reduced S groups in the F1 HPOA. The lack of a DOM concentration dependence does not necessarily implicate one photolysis pathway (direct or indirect) over the other. If the reduction was due to a direct photoprocess, adding additional DOM beyond the minimum needed to bind Hg(II) to strong thiol sites only increases inner filter effects; no change in binding or formation of additional Hg(II):S chromophores would occur. The filter effects would be minimal at the DOM concentrations and short optical path length (<1 cm) used in this study. Likewise, once the minimum DOM concentration needed to strongly bind all of the Hg(II) to thiol sites is reached, additional DOM may not impact indirect photolysis rates. This is due to the high concentrations of some PPRIs in close proximity to DOM molecules where the PPRIs are produced [12, 18-20]. Because all of the Hg(II) is bound to and accesses the high local PPRI concentrations near the DOM, PPRIs produced by additional DOM would have a negligible impact on the PPRI concentrations witnessed by the DOM-bound Hg(II).

The Hg(II) photoreduction kinetics were measured in solutions containing a wide range of DOM types. Because all solutions were prepared to give the same low $A_{310\ nm}$ (0.05 cm^{-1}), light attenuation caused by the DOM in these experiments is insignificant in the 1-cm tubes at this wavelength [21, 22]. Any small inner filter effects would be similar across all of the samples over the wavelength range where the Hg(II):S chromophores absorb. For every DOM experiment, more than enough thiol sites were available to bind Hg(II) in the strong binding regime. When irradiated with simulated solar irradiation at 765 W m^{-2}, Hg(II) reduction

half-lives ranged from 1.5 – 5 hours for the DOM isolates (Figure 3), depending on the nature of the added organic matter. Most fell into a relatively narrow range of 2 – 3 hours, with a peat humic acid being the lone organic matter yielding a half-life > 3 hours. The fact that a diverse range of DOM isolates photoreduced Hg(II) with similar rate constants is consistent with direct photolysis of Hg(II):S chromophores (which are likely to be similar for the DOM samples), but does not rule out intra-DOM indirect photochemistry.

Effects of thiol ligands on Hg(II) photoreduction

To further probe the mechanisms for photoreduction of Hg(II), experiments were conducted using a combination of thiol compounds and DOM. By adding a thiol compound at a concentration of >10^4 times that of the reduced S sites on the DOM, the goal was to transfer Hg(II) from the DOM to the simple thiol ligand and observe the impact on the Hg(II) photoreduction kinetics. The simple thiol ligands and reduced RS^- site on the DOM are predicted to have similar binding constants with Hg(II) [2]. Results shown in Figure 4a-c lend support for a direct photoreduction mechanism of Hg(II). These results show little change in photoreduction rate between experiments conducted with DOM alone, thiol compounds alone, or with a combination of DOM and simple thiol compounds. Figure 4a shows that photoreduction rate for a DOM isolate (5 mg L^{-1}) from the Florida Everglades (F1 HPOA; hydrophobic organic acid fraction) and the same isolate with 10 μM mercaptoacetic acid (MAA) added to solution. Figure 4b shows photoreduction experiments with F1 HPOA and MAA irradiated separately.

The half-life for Hg(II) reduction with MAA was 44 minutes, much shorter than with other thiol model compounds. Photoreduction half-lives of 3 hours were measured with glutathione, L-cysteine, and N-acetyl-L-cysteine as thiol ligands (Figure 4c). This difference in photoreduction rate observed for MAA relative to the other thiols can be explained by the greater increase in absorption in the solar region upon binding Hg(II), as seen in Figure 1. In experiments with these model compounds, there is no photosensitizer present capable of absorbing the radiation and producing reactive intermediates. Therefore, the rapid photoreduction rates that were observed in these experiments must be due to a direct photolysis mechanism in which the Hg:thiol bond itself absorbs the radiant energy, leading to heterolytic bond cleavage and Hg(II) reduction. By extension, it is reasonable to expect that Hg(II) bound to similar strong-binding thiol sites within DOM would also be prone to direct photoreduction. Si and Ariya reported similar results in the photolysis of Hg(II) complexed by simple alkanethiols [17]. Our results expand the scope of thiols capable of inducing Hg(II) photoreduction to include more functionalized species. Furthermore, we show that the UV spectra of the Hg(II):thiol complex and photoreduction rate depend on the identity of the thiol.

Taken together, the results presented in this study point toward direct photolysis being responsible for the reduction of Hg(II) in irradiated DOM solutions. The lack of a DOM concentration dependence on photoreduction, the similar photoreduction rates observed for a wide variety of DOM isolates, and the observed UV spectra and photoreactivity of Hg(II):thiol complexes are all consistent with direct photolysis of Hg(II)-S chromophores. While intra-DOM indirect photochemistry could plausibly explain the results with DOM, it cannot account for the rapid photoreduction of the simple Hg(II):thiol complexes.

Effects of DOM, thiol ligands, and irradiation wavelength on $MeHg^+$ photodemethylation

Photolysis experiments with $MeHg^+$ were conducted in the same way and for the same reasons as in the Hg(II) studies. Figure 2 shows $MeHg^+$ photodemethylation rates at various concentrations of SRFA (5 – 30 mg L^{-1}) and PLFA (5 – 20 mg L^{-1}). Similar to the Hg(II) photoreduction results, $MeHg^+$ photodemethylation occurred relatively rapidly and with no dependence on DOM concentration. Since a direct photolysis mechanism is improbable for MeHg-S bonds (they do not appreciably absorb solar light; Figure 1), the lack of a $MeHg^+$ photodemethylation dependence on DOM concentration is likely due to other factors as shown in multiple studies [1, 3, 9-12]. Experiments with MAA and GSH ligands in the absence of DOM confirmed that these simple $MeHg^+$:thiol complexes indeed have low direct photodemethylation rates, as shown in Figures 4d-e. The direct $MeHg^+$ photodemethylation for MAA (photodemethylation $t_{1/2}$ = 15 h) and GSH (photodemethylation $t_{1/2}$ = 13 h) are much slower than for $MeHg^+$:DOM solutions.

From Figure 2, it is clear that DOM concentration is not the limiting factor controlling photodemethylation in these laboratory experiments over the studied concentration range. Other limiting factors could be light/energy, PPRI concentration, or $MeHg^+$ concentration. Light could be a limiting factor if DOM is shading the inner part of the reaction vessel. This shading is insignificant in the 1-cm quartz tubes at the DOM concentrations used. Higher concentrations of DOM could potentially lead to more production of PPRIs in the bulk solution, but DOM could also act as a quencher for these species. Equal amounts of $MeHg^+$ were spiked into the solutions and more DOM dilutes $MeHg^+$ per unit of DOM, but this did not impact the rate. In addition, if the photodemethylation mechanism occurs in close proximity or is intra-DOM [10, 11], then the concentration of DOM in the bulk solution is irrelevant if shading is insignificant. Thus, it seems the limiting factor in these experiments is simply the concentration of $MeHg^+$ bound to reduced S sites.

The reduced sulfur to $MeHg^+$ ratio in these experiments is high and binding of $MeHg^+$ was predicted to be dominated by reduced sulfur sites for all concentrations of DOM in Figure 2. For example, SRFA is 0.44% S and assuming 47% of S exists as reduced S [23] leads to a reduced S concentration of 3.2×10^{-7} M at the lowest experimental DOM concentration of 5 mg L^{-1}. $MeHg^+$ concentration was a maximum of 1.0×10^{-9} M.

Figures 4d-e shows that photodemethylation kinetics were fastest when the $MeHg^+$ was attached to DOM, slowest when bound to thiol compounds, and intermediate when thiol compounds and DOM were both present. Figure 4d demonstrates the contrast in photodemethylation when only DOM or only simple thiols are present. Qian et al.[10] also found that $MeHg^+$ bound to non-aromatic thiols experienced slower photodemethylation than $MeHg^+$ attached to DOM or aromatic thiols; Tai et al. [11] reported slower photodemethylation for $MeHg^+$ bound to dithiothreitol, but similar photodemethylation rates for $MeHg^+$ bound to DOM or cysteine. Both studies concluded that an intramolecular mechanism was responsible for photodemethylation with light being absorbed by DOM followed by energy transfer and breaking of the C-Hg bond [10, 11].

Figure 4e demonstrates how photodemethylation rates change as $MeHg^+$ is transferred from a thiol ligand to thiols on DOM. A very low rate of photodemethylation is observed when only the thiol is present (10 μM MAA or 2.5 μM GSH); photodemethylation rates increase and then plateau as [DOM] increases while holding the simple thiol ligand concentration constant. Unlike photoreduction of Hg(II), where it did not matter whether Hg was bound to a thiol or DOM, the photodemethylation rate increases when $MeHg^+$ is transferred from the ligand to the DOM. In experiments with only PLFA (5 to 20 mg L^{-1}) present, photodemethylation rates ranged from 6.5 – 7.2 x 10^{-3} min^{-1} (Figure 2) which are similar to the PLFA+GSH experiments between 10 and 30 mg L^{-1} PLFA (Figure 4e). PLFA+MAA experiments never achieved the maximum photodemethylation rate with only PLFA present (all photodemethylation rates from PLFA = 10 to 30 mg L^{-1} are significantly different ($p<0.05$) except GSH+PLFA10 and MAA+PLFA20). These results would support an intramolecular mechanism for photodemethylation with light being absorbed by DOM followed by energy transfer and breaking of the C-Hg bond [10, 11]. It should be noted that $MeHg^+$ bound to simple thiols can also be demethylated by indirect photolysis via PPRIs produced from DOM. In this case, the concentrations of PPRIs such as $^1O_2$ and ^{3}DOM available for reaction by the $MeHg^+$:thiol complexes would be lower than the concentrations of PPRIs observed by $MeHg^+$:DOM complexes undergoing intra-DOM processes.

Experiments using different irradiation wavelengths supported the idea that different photodemethylation rates depend on whether $MeHg^+$ is attached to DOM or a non-aromatic thiol ligand. When comparing $MeHg^+$ photodemethylation obtained for a given irradiation source (UVB, UVA, and broadband), the fastest rates were always found when only DOM was present. Direct comparison between experiments with *different* lamps (broadband, Sunset XLS+; UVA, Luzchem; and UVB, Luzchem), is precarious since the lamps have different intensities and obviously emit different (but overlapping) wavelengths of light. The UVA and UVB lamps have similar irradiances and were operated in the same photoreactor, so the results obtained with these lamps can be compared in a straightforward manner. As seen in Table 3, photodemethylation rates for

a given sample condition were greatest under UVB irradiation relative to UVA, which is consistent with other prior reports [1, 3, 13]. Relative photodemethylation rates ($k_{photodemethylation, UVB}/k_{photodemethylation, UVA}$) for a given sample condition ranged from 4.7 to 19. It should be mentioned, however, that in natural waters longer wavelengths become progressively more important in relative contribution to $MeHg^+$ photodemethylation as depth increases, despite the lower inherent rate of photodemethylation at longer wavelengths, because UVB is filtered by DOM more readily than UVA light [1, 13].

Addition of thiols to PLFA photolysis solutions had a prominent effect on photodemethylation rates in the UVB and UVA experiments (Table 3). Under UVB irradiation, photodemethylation half-lives increased by factors of 2.5 and 1.9 upon addition of MAA and GSH to PLFA solutions, respectively. With UVA light, addition of MAA and GSH to PLFA solutions gave half-lives that were 2.5 and 6.5 times longer than when PLFA was irradiated alone. It is clear that addition of thiols to DOM solutions decreases in photodemethylation rates due to transfer of the $MeHg^+$ to the small thiol compounds. These trends are consistent with an intra-DOM indirect photolysis process that leads to demethylation. The added thiols remove some or all of the $MeHg^+$ from the DOM, resulting in slower rates when the $MeHg^+$ is not attached to the DOM.

Estimation of log *K* for $MeHg^+$ binding to DOM

Assuming virtually all the $MeHg^+$ has been transferred from GSH to PLFA when the maximum photodemethylation rate is achieved at 10 mg L^{-1} PLFA, a binding constant between $MeHg^+$ and PLFA can be estimated by assuming 50% has been transferred at half that concentration. Half of the maximum photodemethylation rate is also achieved at approximately 5 mg L^{-1} PLFA (Figure 4e). Making these initial assumptions and using literature values to estimate the unprotonated thiol concentration on PLFA and GSH, a log *K* value for $MeHg^+$ binding to RS^- sites on PLFA was estimated as:

$$MeHg^+ + {}^-SR \rightarrow MeHgSR \qquad \log K = 16.7$$

The key literature values needed for the estimates were log K of 15.99 [24] for $MeHg^+$ binding to GSH, pK_a = 9.69 for GSH [24], and pK_a = 10 for thiol sites on PLFA [2]. PLFA has 3.03% S and 69% of the sulfur is reduced S, of which 30% is assumed to be thiol [25, 26]. No other ligands on the DOM or in solution were relevant for the binding of $MeHg^+$. The assumption that 50% of the $MeHg^+$ is on the PLFA at the 5 mg L^{-1} experiment is not strictly valid in the dynamic conditions occurring throughout the five-hour experiments. Equilibrium is assumed at the beginning since the solution was allowed to equilibrate overnight and others have assumed less than one hour is sufficient [3]. However, while the experiment is underway, the $MeHg^+$ attached to DOM (k = 6.2 x 10^{-3} min^{-1}) would undergo photodemethylation faster than $MeHg^+$ attached to GSH (k = 8.6 x 10^{-4} min^{-1}) leading to non-equilibrium. $MeHg^+$ migration off of GSH and towards DOM would be favored to try to

reach equilibrium. Assuming $MeHg^+$ was initially distributed equally between GSH and PLFA (5 mg L^{-1}/10 μM GSH), simple equilibrium and non-equilibrium models were run and compared to the experimental data (Figure 5). The non-equilibrium model assumed the system did not attempt to reach equilibrium during the five-hour experiment and the rate constants listed above for $MeHg^+$ attached to DOM or GSH did not change. Alternatively, it was assumed that equilibrium conditions were maintained throughout the experiments (Figure 5). The models diverge after a few hours and the non-equilibrium model overestimated the final concentrations slightly more than the equilibrium model. The best fit to the experimental data was found using an equilibrium model with 40% initially on DOM.

An estimated log *K* of 16.7 at pH 7 for $MeHg^+$ binding with thiols is in line with values found for simple thiols [24, 27] and the few experimental values reported for $MeHg^+$ binding to reduced S in DOM [25, 28, 29]. Karlsson and Skyllberg [28] used a competitive exchange approach and determined log *K* ranging from 15.6 to 17.1 at pH ranging from 5.1 down to 2.0. Qian et al.[25] also used a competitive binding technique and estimated log *K* to range from 16.3 to 17.1 at pH 3.8. Khwaja et al. [29] reported log *K* ranging from 15.5 to 16 using a competitive ligand, equilibrium dialysis technique. Further experiments with multiple ligands at finer concentration increments would ideally be used to better estimate a log *K*, but here we demonstrate the potential utility of using different photodemethylation rates between $MeHg^+$ associated with DOM or GSH to estimate a binding coefficient.

Analysis of possible indirect reaction pathways for $MeHg^+$ photodemethylation

Experiments were conducted where quenchers of specific PPRIs were added or removed to assess the potential importance of various PPRIs on $MeHg^+$ photodemethylation. Results of experiments comparing the photodemethylation rate for PLFA solutions that were air-saturated to those that had been deoxygenated with N_2 are shown in Figure 6. A slight rate enhancement is observed when oxygen is removed from the system. This result is consistent with the indirect photochemical reaction initiating from a ^{3}DOM, since oxygen is a potent quencher of excited state triplets. It is possible, however, that the photodemethylation process proceeds via multiple mechanisms. Deoxygenation would prevent the sensitized formation of $^1O_2$ (which occurs when dissolved oxygen quenches ^{3}DOM), and demethylation due to $^1O_2$ would be insignificant in this case. The enhancement upon removal of oxygen from the system is rather small, and it is possible that in the aerated sample reactions initiated by $^1O_2$ and ^{3}DOM both occur. Prior studies separately implicate $^1O_2$ and ^{3}DOM in $MeHg^+$ photodemethylation [10, 12].

To further explore the potential role of $^1O_2$ in the photodemethylation process, an experiment was performed to measure the reactivity of $MeHg^+$ with $^1O_2$ formed in a non-photochemical reaction where $^1O_2$ is

produced in the absence of ^{3}DOM [30]. In this experiment $MeHg^+$ (with MAA as ligand) and the $^1O_2$ probe molecule furfuryl alcohol (FFA) were placed in the same reaction vessel and exposed to $^1O_2$ produced from the molybdate-catalyzed disproportionation of H_2O_2 [15]. The $MeHg^+$ was complexed with MAA to model the $MeHg^+$-S bond as found in a DOM environment. As seen in Figure 7, no change was observed in $MeHg^+$ concentration over the course of the experiment, while FFA was significantly degraded by $^1O_2$. Because the rate of $MeHg^+$ demethylation was shown to be negligible, it must have a relatively slow rate of reaction with $^1O_2$.

To determine whether $^1O_2$ may still be involved in $MeHg^+$ photodemethylation despite its low reactivity with $^1O_2$, we explored the effect that microheterogeneous $^1O_2$ distributions may have on $MeHg^+$ bound to DOM. This involved measuring $[^1O_2]_{SS}$ in the aqueous phase and then used known relationships to estimate the $^1O_2$ expected in the DOM phase. The loss of FFA with 10 mg L^{-1} PLFA gives k_{obs} = 0.1.1 x 10^{-4} s^{-1} at pH 7, which can be converted to $[^1O_2]_{SS}$ by dividing it by the bimolecular rate constant of reaction between $^1O_2$ and FFA ($k_{FFA,1O2}$ = 8.3 x 10^7 $M^{-1}s^{-1}$) [31]. This analysis gives a $[^1O_2]_{SS}$ value of 1.3 pM in the bulk aqueous phase that the FFA monitors. In the $MeHg^+$ experiments with PLFA and no additional ligands, the $MeHg^+$ is expected to be bound to the PLFA, where apparent $^1O_2$ concentrations are expected to be much higher than in the aqueous phase. A study by Grandbois, et al. [18] measured relative $[^1O_2]_{SS}$ in the aqueous phase $[^1O_2]_{aq}$ and in the DOM phase $[^1O_2]_{aq}$. They measured $[^1O_2]_{DOM}$ = 2,700 fM and $[^1O_2]_{aq}$ = 1.7 fM at 1 mg DOC/L PLFA. At low DOM concentrations, the $[^1O_2]_{aq}$ scales directly with [DOM]. We can convert the 10 mg L^{-1} concentration of PLFA used in our experiment to mg DOC/L by accounting for the percent composition of carbon in PLFA (52.5 %). This gives 5.25 mg DOC L^{-1}, and the expected $[^1O_2]_{aq}$ at this concentration in the Grandbois, et al. study would be 8.8 fM (1.7 fM x 5.25). The enhancement in $[^1O_2]$ in the DOM phase at this concentration is thus 2,700 fM/8.8 fM = 300. With this enhancement ratio and the $[^1O_2]_{aq}$ measured by FFA in our experiments, we calculate a $[^1O_2]_{DOM}$ in our 10 mg L^{-1} PLFA experiment to be 390 pM. We can use the observed photodemethylation demethylation rate constant (k_{obs} = 0.000113 s^{-1}) at this PLFA concentration and the $[^1O_2]_{DOM}$ value estimated above to determine what the $MeHg^+$ rate constant ($k_{MeHg,1O2}$) must be if the photodemethylation was due entirely to $^1O_2$ ($k_{MeHg,1O2} = k_{obs}/[^1O_2]_{DOM}$). This treatment gives $k_{MeHg,1O2}$ ~ 3 x 10^5 $M^{-1}s^{-1}$. This is a relatively slow rate constant that would likely be unmeasurable under the conditions used in the H_2O_2 disproportionation experiment (since the slope of the $MeHg^+$ loss would be ~300 times lower than that of FFA based on the known $k_{FFA,1O2}$ and the maximum $k_{MeHg,1O2}$ value estimated above). To summarize these results, $MeHg^+$ has a slow $k_{MeHg,1O2}$, but due to the elevated $[^1O_2]$ within and near DOM, some contribution by $^1O_2$ in $MeHg^+$ cannot be ruled out based on our results.

To better understand how $MeHg^+$-S react with various PPRIs, additional quenching experiments were performed for solutions containing both PLFA and simple thiols. Figure 6b shows these results. As in the case of PLFA experiments performed in the absence of thiol ligands, removal of oxygen led to rate enhancements relative to those seen in aerated solutions. Again, this points to the involvement of ^{3}DOM in the indirect photodemethylation process. The involvement of a process initiated by ^{3}DOM is further supported by a decrease in photodemethylation rate when the triplet quencher sorbic acid (SA, 1 mM) is added to solution. These data do not necessarily rule out some involvement by other processes, however. Addition of the $^1O_2$ quencher sodium azide led to a substantial decrease in photodemethylation rate, which is difficult to explain based on the expected low reactivity of $MeHg^+$ and the low $[^1O_2]_{SS}$. Based on the $k_{MeHg,1O2}$ estimated above and the $[^1O_2]_{aq}$ determined by the FFA probe, reaction of $MeHg^+$:thiol complexes in the aqueous phase would have a photodemethylation $t_{1/2}$ on the order of 500 h ($t_{1/2}$ = ln2/[(3 x 10^5 $M^{-1}s^{-1}$)(1.3 x 10^{-12} M)(60 s min^{-1})(60 min h^{-1})]) due to $^1O_2$ in the aqueous phase, *even in the absence of an added $^1O_2$ quencher*. An experiment with 1 % v/v added isopropanol (iPrOH), a potent ·OH quencher, did not influence the photodemethylation rate, thus ruling out the influence of ·OH in the demethylation process.

St. Louis River field study

Important fundamental differences exist between photochemical studies performed in the laboratory versus the field. For example, DOM attenuates the penetration of light into water bodies limiting the photic zone as DOM concentrations increase. In the laboratory, where experiments are conducted in light chambers with small-diameter containers, inner filter effects tend to be less important than in the field. In the laboratory experiments described above, inner filter effects on the rate of $MeHg^+$ photodemethylation was negligible due to the small (1 cm) diameter of the quartz tubes. We performed $MeHg^+$ photodemethylation experiments in a highly colored surface water where light attenuation reduces photodemethylation rates at depth.

Figure 8 details a three-day study conducted on the St. Louis River from August 7-9, 2013. August 7 was a partly sunny day with high cumulus clouds covering about 50% of the sky. St. Louis River water at the time had a DOC concentration of about 35 mg L^{-1}. The spiked $MeHg^+$ concentrations are 10-15 times higher than ambient levels at this time of year, but at these levels, all the $MeHg^+$ is predicted to be bound to reduced sulfur sites on DOM. Assuming S constitutes 0.2% of C in the DOM [2], the concentration of thiol sites is estimated to be ~ 2 µM compared to the spiked $MeHg^+$ of 75 pM. As Lehnherr and St. Louis [13] have shown and others have surmised[3], $MeHg^+$ photodemethylation rates in spike experiments should be equivalent to those at ambient levels if the $MeHg^+$ to DOC concentrations are low enough to ensure binding is dominated

by reduced S sites. Our experiments fall well within the strong reduced S binding regime. Dark bottles collected before and after the 4-hr experiment demonstrated that biological degradation was insignificant.

Photodemethylation was minimal below the surface as no changes in $MeHg^+$ concentration were observed over 3 days at depths of 10, 20, and 40 cm. An unusually low $MeHg^+$ concentration was observed for the first time point collected (1 h) for the surface sample. Given that the samples were spiked to nominal concentrations of 15 ng/L and other time points for the surface sample displayed a consistently different kinetic profile, it is likely this point is an outlier, but there were no analytical or procedural reasons to remove the data point. If one ignores the t= 1 sample from the surface series, the concentration decreased to 6.6 ng L^{-1} after 3 days (~50 % of the spike concentration). An initial concentration was not measured in the quartz tubes, but using the $MeHg^+$ concentration at 40 cm depth, the initial concentration was 13.5 ng L^{-1}.

These data show that while photodemethylation is expected to be a significant loss process at the surface of St. Louis River, photodemethylation rates decrease precipitously with depth. This is a common photochemical phenomenon due to the substantial light attenuation brought about by the highly absorbing St. Louis River water. Lehnherr and St. Louis [13] found little photodemethylation below 50 cm in a lake with 'high' DOC of 12.8 mg L^{-1}. At 35 mg L^{-1} DOC, the inner filter effect is quite large for the St. Louis River, and our data from experiments performed at depth reflect this expectation. It is expected, however, that as the water flows downstream and is diluted and enters Lake Superior (and thus the DOC content and inner filtering decreases), photodemethylation will become a significant $MeHg^+$ loss process at deeper depths.

V. Conclusions

Our results suggest that Hg(II) photoreduction and $MeHg^+$ photodemethylation depend on binding to DOM, particularly to thiol sites within the DOM. Both photoprocesses are expected to occur rapidly at near surface depths, but field results for $MeHg^+$ photodemethylation show that photolysis rates drop precipitously with depth in highly colored natural waters. In the case of Hg(II), direct photolysis of Hg(II):thiol chromophores appear to be responsible for the observed photoreduction, which is in line with prior research[17]. Our results suggest that the structure of the thiol that binds the Hg(II) impacts both the amount of solar light absorbed by the complex and the photoreduction rate. Absorption spectra of $MeHg^+$:thiol complexes showed little to no overlap with the solar spectrum, ruling out direct photolysis of $MeHg^+$:thiol chromophores as a significant photodemethylation pathway. The lack of a DOM concentration dependence on $MeHg^+$ photodemethylation rates implicated an intra-humic indirect photolysis pathway whereby $MeHg^+$ loss is ascribed to reaction with energy transfer from other DOM chromophores or PPRIs generated within the DOM molecules. Results from

studies where concentrations of various quenchers of specific PPRIs implicate ^{3}DOM in the photodemethylation process, though reaction with $^1O_2$ cannot be ruled out despite the low inherent reactivity of $MeHg^+$ with $^1O_2$

Acknowledgements:

We thank Tina Dahlseid, Anna Huff, Nathan Olson, Will Metcalf, Michael Walker, Alison Agather, and Bryan Voigt for assistance with methylmercury analysis and collection of field samples, and Kenna Butler (USGS) for her assistance obtaining organic matter isolates. Travis Bavin and Mike Berndt provided valuable technical assistance and site selection suggestions. Funding was provided by the Minnesota Department of Natural Resources Iron Ore Cooperative Research program, the MN DNR Environmental Cooperative Research program, the Clean Water Fund through the Minnesota Pollution Control Agency, the National Science Foundation (Research award number 0923430), Gustavus Adolphus College, Seattle University and the U. S. Geological Survey Toxics Substances Hydrology Program. Any use of trade, firm, or product names is for descriptive purposes only and does not imply endorsement by the U.S. Government.

VI. References

1. F. J. Black, B. A. Poulin and A. R. Flegal, *Geochim. Cosmochim. Acta*, 2012, **84**, 492-507.
2. U. Skyllberg, *Journal of Geophysical Research: Biogeosciences*, 2008, **113**, G00C03.
3. C. Fernández-Gómez, A. Drott, E. Björn, S. Díez, J. M. Bayona, S. Tesfalidet, A. Lindfors and U. Skyllberg, *Environ. Sci. Technol.*, 2013, **47**, 6279-6287.
4. R. G. Zepp, P. F. Schlotzhauer and R. M. Sink, *Environ. Sci. Technol.*, 1985, **19**, 74-81.
5. M. Amyot, D. J. McQueen, G. Mierle and D. R. S. Lean, *Environ. Sci. Technol.*, 1994, **28**, 2366-2371.
6. W. Schroeder, O. Lindqvist, J. Munthe and Z. Xiao, *Science of The Total Environment*, 1992, **125**, 47-66.
7. G. Vandal, R. Mason and W. Fitzgerald, *Water Air & Soil Pollution*, 1991, **56**, 791-803.
8. E. Vost, M. Amyot and N. J. O'Driscoll, in *Environmental Chemistry and Toxicology of Mercury*, eds. G. Liu, Y. Cai and N. J. O'Driscoll, John Wiley & Sons, Hoboken, NJ, 2012, ch. 6, pp. 193-218.
9. C. R. Hammerschmidt and W. F. Fitzgerald, *Environ. Sci. Technol.*, 2010, **44**, 6138-6143.
10. Y. Qian, X. Yin, H. Lin, B. Rao, S. C. Brooks, L. Liang and B. Gu, *Environmental Science & Technology Letters*, 2014, **1**, 426-431.
11. C. Tai, Y. Li, Y. Yin, L. J. Scinto, G. Jiang and Y. Cai, *Environ. Sci. Technol.*, 2014, **48**, 7333-7340.
12. T. Zhang and H. Hsu-Kim, *Nature Geosci.*, 2010, **3**, 473-476.
13. I. Lehnherr and V. L. St. Louis, *Environ. Sci. Technol.*, 2009, **43**, 5692-5698.
14. G. R. Aiken, D. M. McKnight, K. A. Thorn and E. M. Thurman, *Organic Geochemistry*, 1992, **18**, 567-573.
15. K. Boehme and H. D. Brauer, *Inorganic Chemistry*, 1992, **31**, 3468-3471.
16. H. Hintelmann and R. Evans, *Fresenius Journal of Analytical Chemistry.*, 1997, **358**, 378-385.
17. L. Si and P. A. Ariya, *Chemosphere*, 2011, **84**, 1079-1084.

18. M. Grandbois, D. E. Latch and K. McNeill, *Environ. Sci. Technol.*, 2008, **42**, 9184-9190.
19. T. Kohn, M. Grandbois, K. McNeill and K. L. Nelson, *Environ. Sci. Technol.*, 2007, **41**, 4626-4632.
20. D. E. Latch and K. McNeill, *Science*, 2006, **311**, 1743-1747.
21. A. Leifer, *The kinetics of environmental aquatic photochemistry: theory and practice*, American Chemical Society: , Washington DC, 1988.
22. G. P. M. Schwarzenbach R. P., Imboden, D. M. , *Environmental Organic Chemistry*, Wiley-Interscience, New York, 2nd edn., 2002.
23. K. Xia, F. Weesner, W. F. Bleam, P. A. Helmke, P. R. Bloom and U. L. Skyllberg, *Soil Science Society of America Journal*, 1998, **62**, 1240-1246.
24. A. P. Arnold and A. J. Canty, *Canadian Journal of Chemistry*, 1983, **61**, 1428-1434.
25. J. Qian, U. Skyllberg, W. Frech, W. F. Bleam, P. R. Bloom and P. E. Petit, *Geochim. Cosmochim. Acta*, 2002, **66**, 3873-3885.
26. A. Manceau and K. L. Nagy, *Geochim. Cosmochim. Acta*, 2012, **99**, 206-223.
27. D. L. Rabenstein and M. T. Fairhurst, *Journal of the American Chemical Society*, 1975, **97**, 2086-2092.
28. T. Karlsson and U. Skyllberg, *Environ. Sci. Technol.*, 2003, **37**, 4912-4918.
29. A. R. Khwaja, P. R. Bloom and P. L. Brezonik, *Environ. Sci. Technol.*, 2010, **44**, 6151-6156.
30. W. R. Haag, J. r. Hoigne´, E. Gassman and A. M. Braun, *Chemosphere*, 1984, **13**, 631-640.
31. D. E. Latch, B. L. Stender, J. L. Packer, W. A. Arnold and K. McNeill, *Environ. Sci. Technol.*, 2003, **37**, 3342-3350.
32. J. L. Weishaar, G. R. Aiken, B. A. Bergamaschi, M. S. Fram, R. Fujii and K. Mopper, *Environ. Sci. Technol.*, 2003, **37**, 4702-4708.

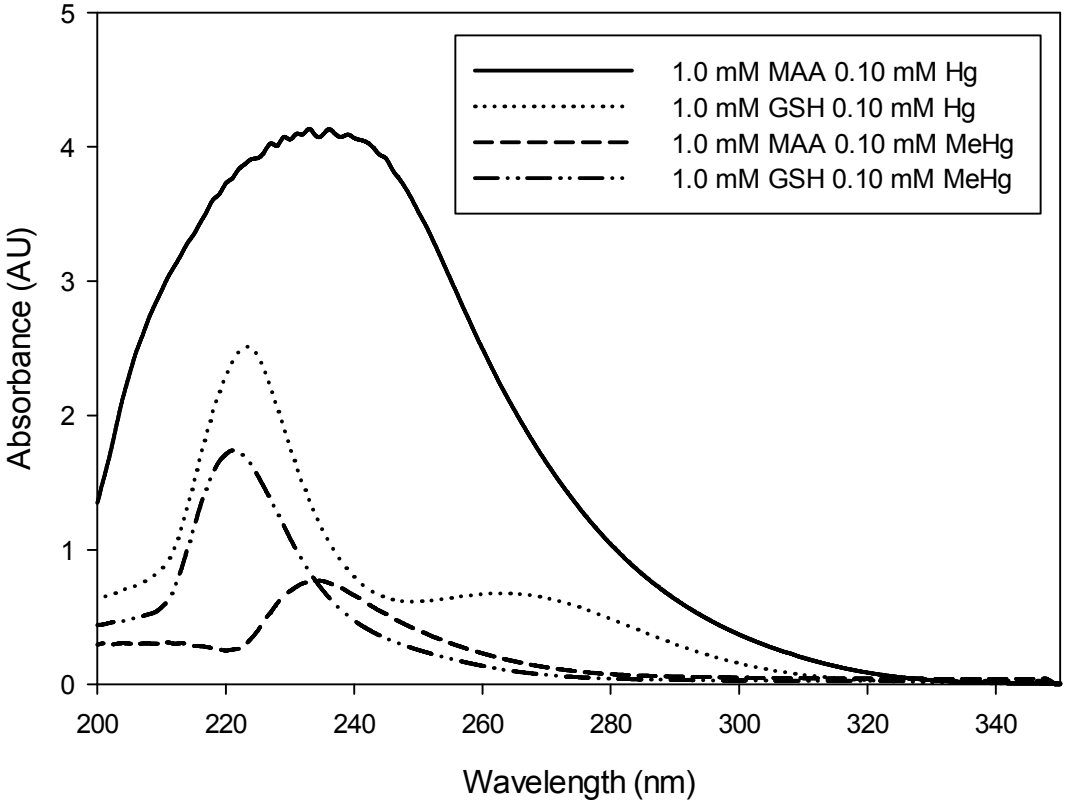

Figure 1. UVspectra for Hg(II) and $MeHg^+$ while bonded to the thiol ligands mercaptoacetic acid (MAA) and glutathione (GSH). Hg(II):thiol complexes are observed to have significant overlap with the solar spectrum above 300 nm while $MeHg^+$:thiol complexes do not.

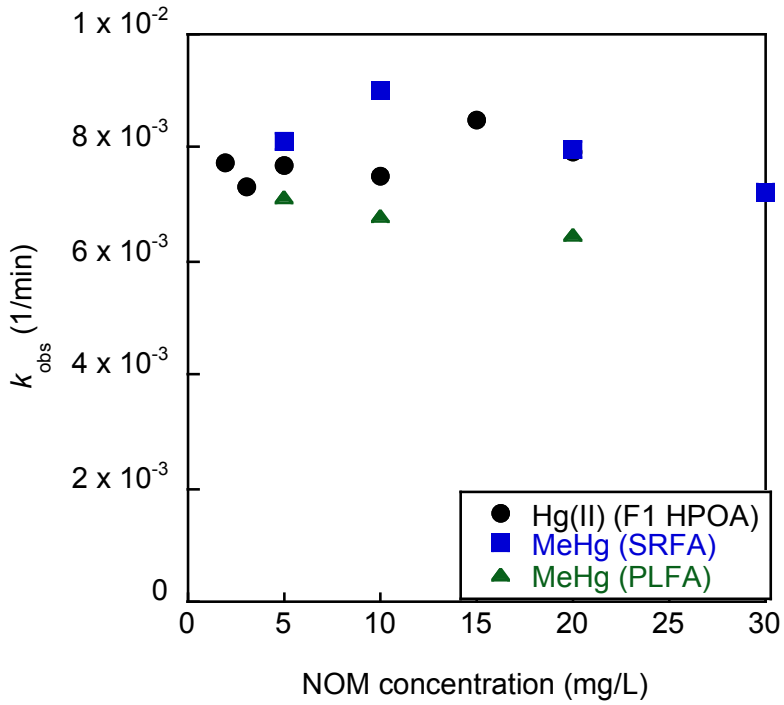

Figure 2. Photoreduction of Hg(II) (black circles) with varying concentrations of a natural organic matter sample isolated from the Florida Everglades (F1 HPOA) and photodemethylation rate constants measured with varying concentrations of SRFA (blue squares) and PLFA (green triangles). All experiments were performed in a solar simulator with a filtered Xe lamp operated at 765 W/m^2

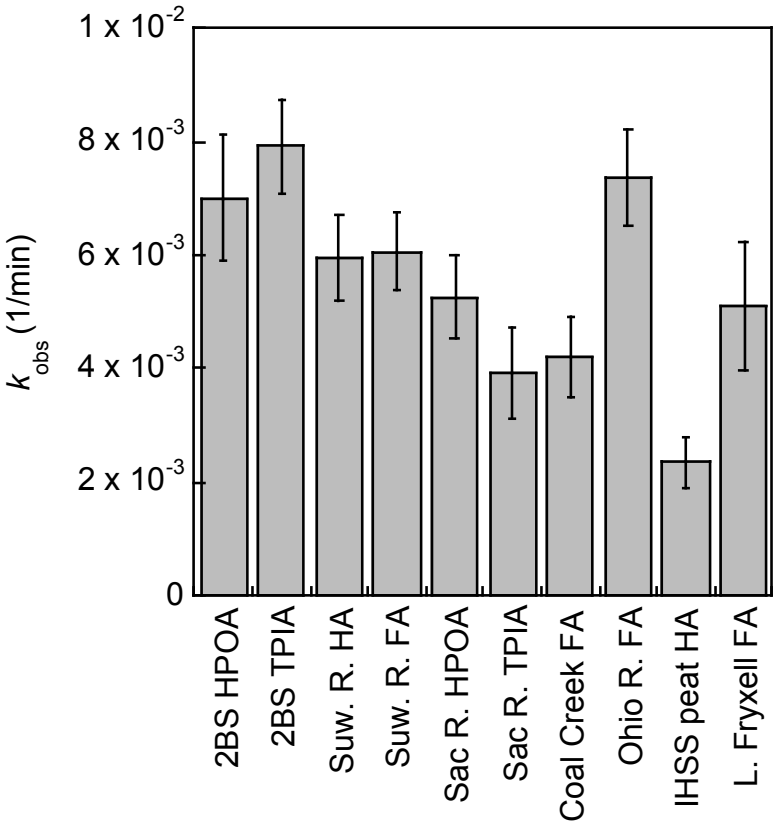

Figure 3. Hg(II) photoreduction rate constants measured in a solar simulator for a variety of DOM isolates. Concentrations of DOM isolates were selected to give $A_{310\ nm}$ = 0.05 (in a 1.0-cm cuvette) so that each sample had the same amount of light filtering where the simulated solar light spectrum and Hg(II):thiol complexes overlapped most strongly. Concentrations used are as follows: 6.9 mg L^{-1} 2BS HPOA, 11.8 mg L^{-1} 2BS TPIA, 2.7 mg L^{-1} Suw. R. HA, 4.9 mg L^{-1} Suw R. FA, 5.1 mg L^{-1} Sac. R. HPOA, 12.2 mg L^{-1} Sac. R. TPIA, 4.1 mg L^{-1} Coal Creek FA, 6.8 mg L^{-1} Ohio R. FA, 2.2 mg L^{-1} IHSS peat HA, and 12.8 mg L^{-1} L. Fryxell FA.

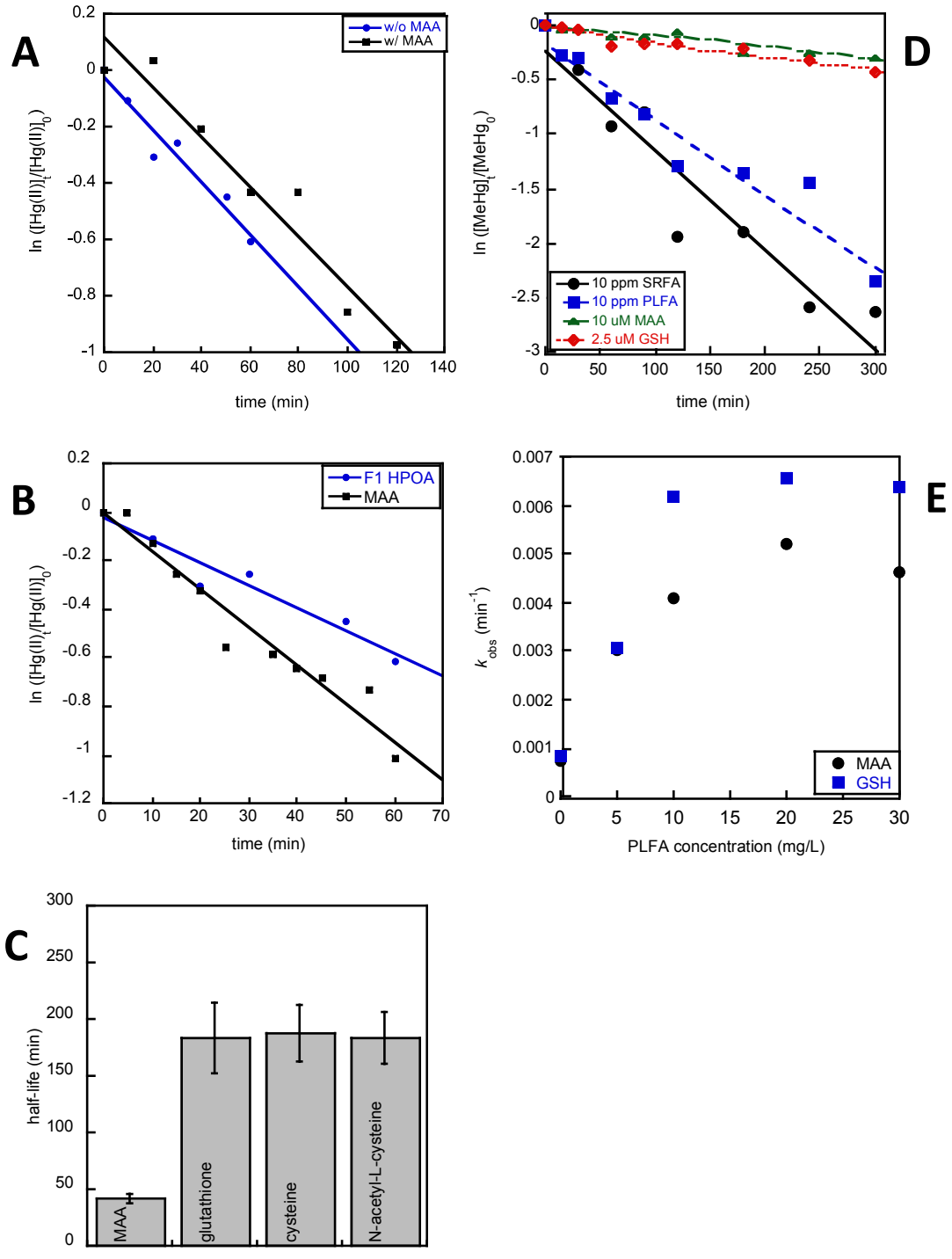

Figure 4. Top left: Hg(II) reduction in solutions of 5 mg L^{-1} F1 HPOA and the absence (blue circles) and presence of mercaptoacetic acid (MAA; 10 μM; black squares). Middle left: Hg(II) photoreduction in solutions of either 5 mg L^{-1} F1 HPOA (blue circles) or 10 μM MAA (black squares). Bottom left: Hg(II) photoreduction half-lives with simple thiol ligands and no DOM present (thiols used are labeled on the bar to which they correspond). Top right: Photodemethylation of MeHg with various ligands added: 10 mg L^{-1} SRFA (black circles), 10mg L^{-1} PLFA (black circles), 10 μM MAA (green diamonds), and 2.5 μM GSH (red diamonds). Bottom

right: Effect of varying PLFA concentration on the photodemethylation of MeHg in solutions containing either 10 μM MAA or 2.5 μM GSH.

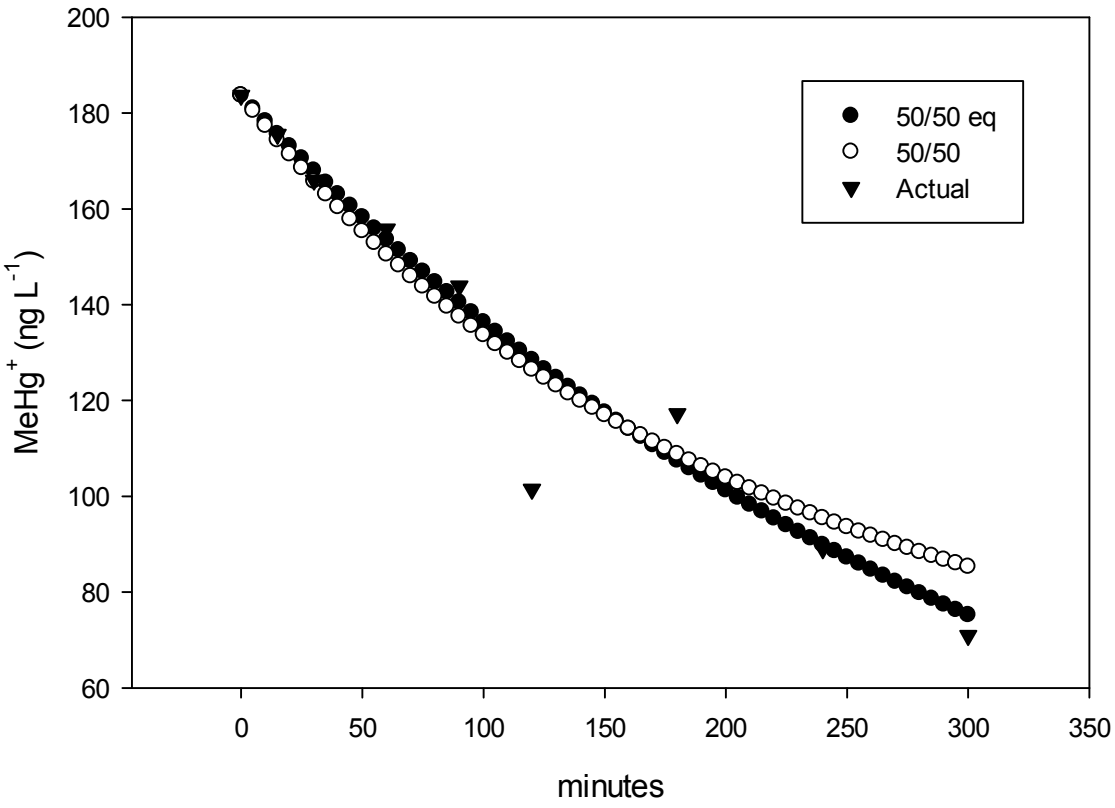

Figure 5. Figure showing modeled $MeHg^+$ concentrations based on an equal distribution of $MeHg^+$ between DOM and GSH at 5 mg L^{-1} PLFA and 10 µM GSH. Triangles are the actual data from the 5 mg L^{-1}, 10 µM experiment. The 50/50 model assumes equilibrium only at the beginning of the experiment. Time points were calculated every 5 minutes assuming first order kinetics with k = 0.00086 min^{-1} for $MeHg^+$ attached to GSH and k= 0.0062 min^{-1} for $MeHg^+$ attached to DOM. The 50/50 equilibrium model assumes that equilibrium is maintained the entire period. The same rate constants were used in both models.

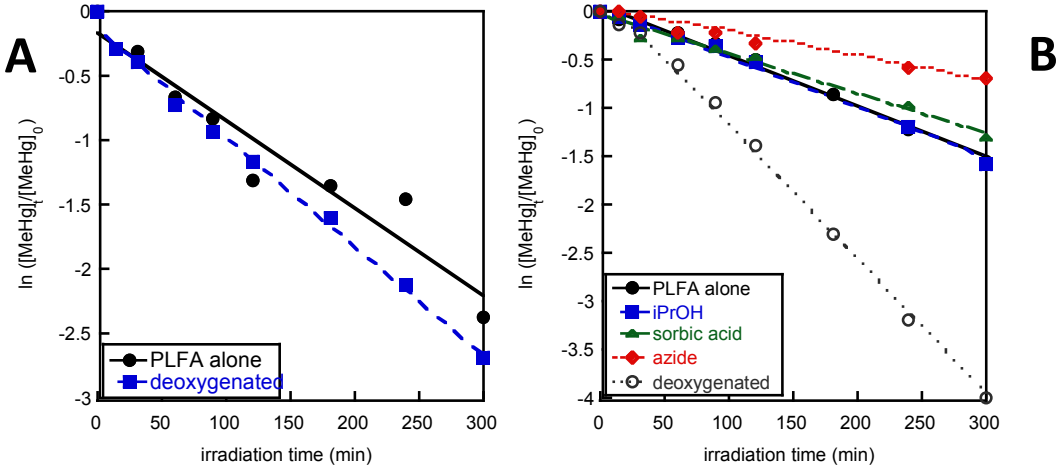

Figure 6. Left panel: Effect of oxygen removal on photodemethylation of MeHg with 10 mg L^{-1} PLFA. Experiments were performed in aerated solutions (black circles) or in N_2-sparged samples (blue squares). Right panel: Effect of various quenchers on MeHg photodemethylation in solutions containing 10 mg L^{-1} PLFA and 10 μM MAA.

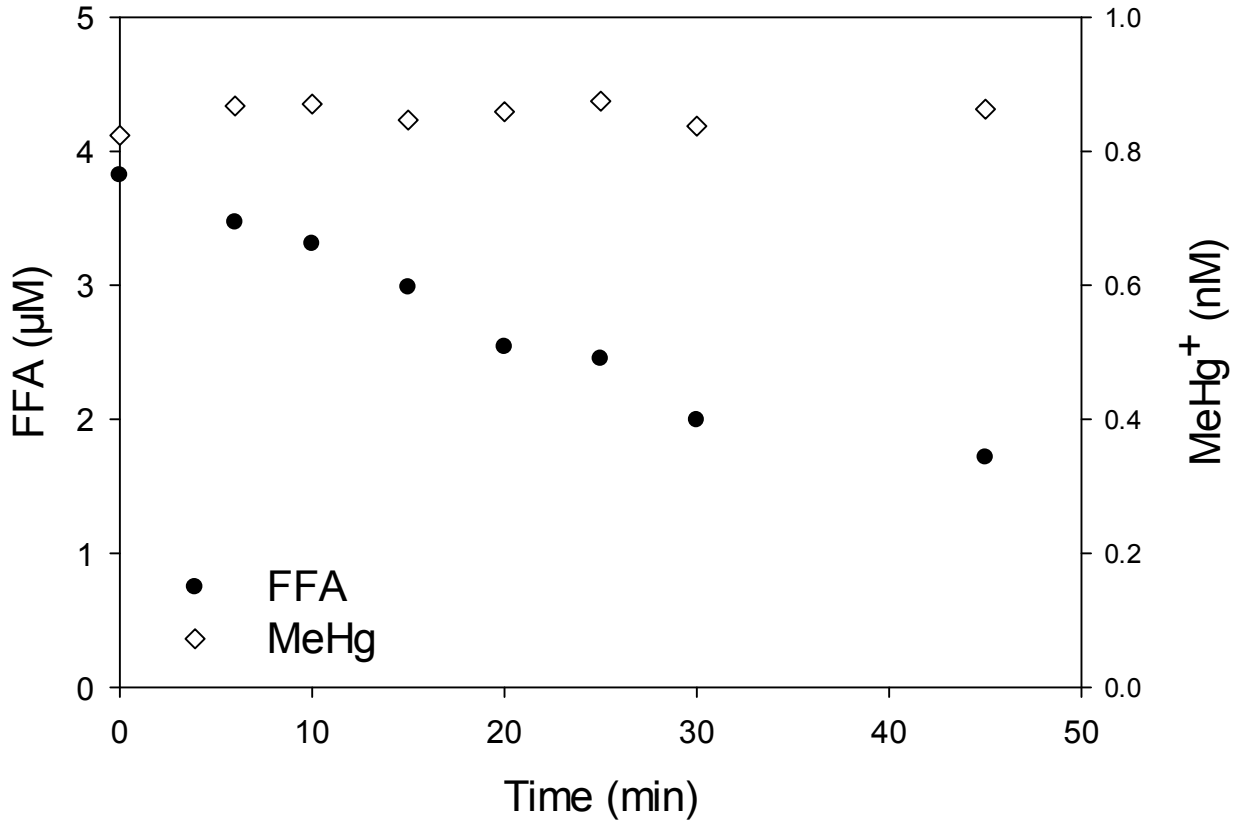

Figure 7. Loss of furfuryl alcohol (FFA) and $MeHg^+$ exposed to $^1O_2$ generated in solution from the molybdate-catalyzed disproportionation of H_2O_2. The $MeHg^+$ shows negligible reaction with $^1O_2$ relative to FFA, a commonly used $^1O_2$ probe molecule.

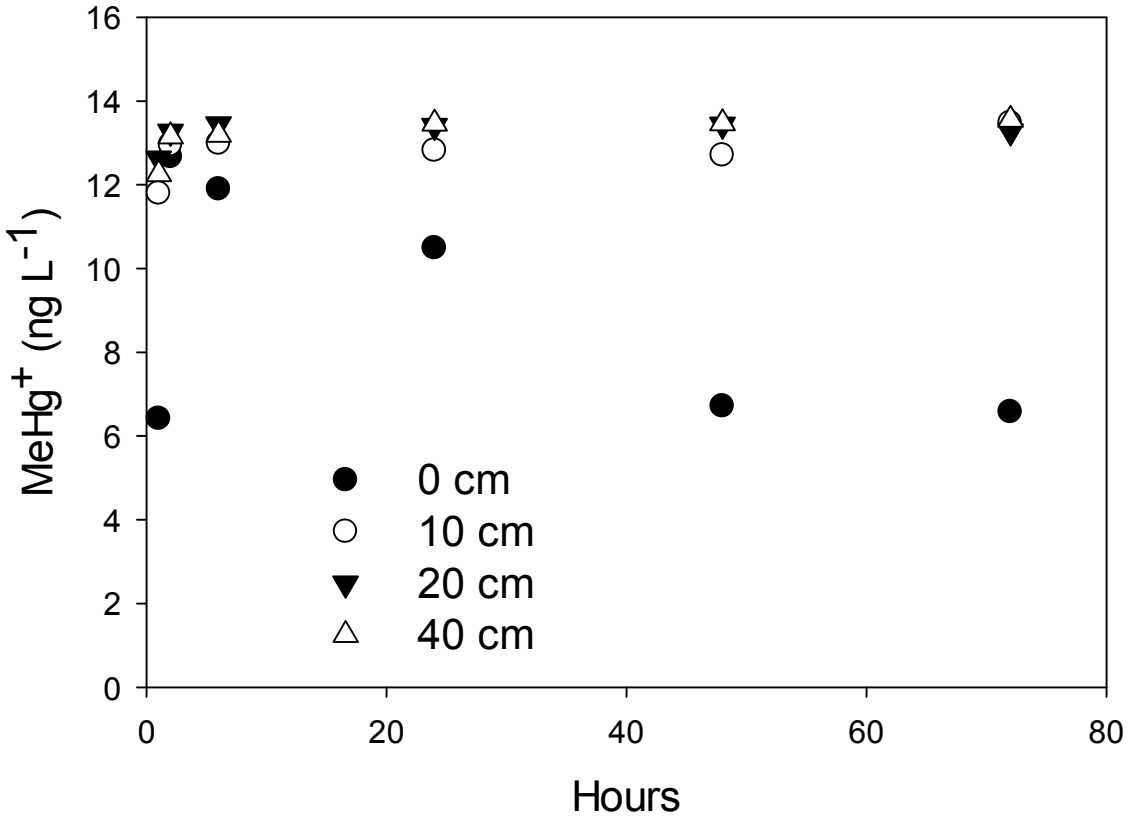

Figure 8. Photodemethylation of $MeHg^+$ in the St. Louis River (MN) in August, 2013.

Table 1. Site Descriptions for Dissolved Organic Matter Isolates.

Sample	Site Description
Suwannee River Humic Acid (SRHA) Suwannee River Fulvic Acid (SRFA)	Black water river draining the Okeefenokee Swamp. Sampled at Fargo, Georgia. Vegetation types: Southern Floodplain Forest (Quercus, Nyassa, Taxodium); International Humic Substances Society (IHSS) standards.
Pony Lake FA (PLFA)	Saline eutrophic lake in Antarctica. Isolate obtained from the IHSS.
Coal Creek Fulvic Acid (CCFA)	Small mountain stream draining the Flattops Wilderness Area, Colorado. Vegetation type: Spruce-Fir Forest (Picea, Abies)
F1 Hydrophobic Acid (F1HPOA)	Eutrophied marshland located in Water Conservation Area 2A in the northern Everglades. Vegetation dominated by cattails. (26.3597" N; 80.3705 W)
2BS Hydrophobic Acid (2BSHPOA) 2BS Hydrophobic Acid (2BSTPIA)	Relatively pristine marshland located in Water Conservation Area 2B in the northern Everglades. Vegetation dominated by saw grass. (26.15 N; 82.375 W)
Ohio River Fulvic Acid (OhRFA)	Major river draining east-central United States. Sampled at Cincinnati, Ohio. Vegetation types: Appalachian Oak Forest, Mixed Mesophytic Forest, Oak Hickory Forest.
Lake Fryxell Fulvic Acid (LFFA)	Ice-covered lake in the McMurdo Dry Valleys, Antarctica. Organic matter dominated by autochthonous sources (algae, bacteria).
Sacramento River HPOA Sacramento River TPIA	Major River in Northern California with headwaters in the Sierra Mountains. Sample collected near Rio Vista, CA. Vegetation types: Mixed Conifer Forest, California Oakwoods,
Pahokee Peat HA (IHSS HA)	The Pahokee peat is a typical agricultural peat soil of the Florida Everglades. Pahokee soils formed in organic deposits of freshwater marshes. The IHSS sample was obtained from the University of Florida Belle Glade Research Station.

Table 2. Chemical Characteristics of Dissolved Organic Matter Isolates.

Isolate	Code	% wt C	H	O	N	S	Ash	% Arom C[a]	$SUVA_{280}$[b]
Suwannee R. Humic Acid	SRHA	53.4	3.9	40.9	1.1	0.7	4.1	35.1	5.47
Suwannee R. Fulvic Acid	SRFA	54.2	3.9	38.0	0.7	0.4	0.19	22.9	3.01
Pony Lake Fulvic Acid	PLFA	52.5	5.4	31.4	6.5	3.0	1.25	nd	1.91
Everglades F1 HPOA	F1 HPOA	52.2	4.64	39.9	1.53	1.73	9.4	25.4	3.09
Everglades 2BS HPOA	2BS HPOA	52.3	4.8	40.2	1.6	1.2	7.3	21.3	2.27
Everglades 2BS TPIA	2BS TPIA	nd	nd	nd	nd	nd	nd	nd	nd[c]
Sacramento River HPOA	Sac R. HPOA	51.4	5.3	40.3	2.0	0.9	17.3	nd	nd
Sacramento River TPIA	Sac R. TPIA	nd	nd	nd	nd	nd	nd	nd	nd
Coal Creek FA	CCFA	52.8	4.5	38.4	1.0	0.7	1.23	28.0	3.16
Ohio River Fulvic Acid	Ohio R. FA	55.5	5.4	35.9	1.5	1.3	0.6	24.3	2.17
Pahokee Peat Humic Acid	IHSS Peat HA	56.4	3.8	37.3	3.7	0.7	1.1	47	nd
Lake Fryxell Fulvic Acid	L. Fryxell FA	55.0	5.5	34.9	3.3	1.2	2.3	15.2	1.41
Manganika Lake HPOA	LMHPOA	52.2	4.6	40.4	1.7	1.1	3.8	26.3	nd
St. Louis River HPOA	SLRHPOA	51.4	4.2	42.7	1.2	0.5	2.6	27.5	nd

[a] % arom C = % aromatic carbon as determined by ^{13}C nuclear magnetic resonance spectroscopy (integrated peak area from δ 110 – 160 ppm relative to the integrated area across the entire spectrum)

[b] $SUVA_{280}$ = specific UV absorbance at 280 nm ($SUVA_{280} = A_{280\,nm}/[DOC]$ in units of L $mg^{-1}m^{-1}$) [32]

[c] nd = not determined

Table 3. Effect of Irradiation Source on Photodemethylation Half-Lives (Photodemethylation $t_{1/2}$) and Relative Photodemethylation Rates

	photodemethylation $t_{1/2}$ (min)		relative photodemethylation rate
Sample[a]	UVB	UVA	($k_{PD, UVB}/k_{PD, UVA}$)
PLFA[a]	30 ± 1	140 ± 10	4.7
PLFA + MAA[b]	74 ± 3	350 ± 30	4.7
PLFA + GSH[c]	58 ± 3	910 ± 80	16
MAA[d]	170 ± 10	3100 ± 700	19
GSH[e]	97 ± 3	1600 ± 100	17
Saint Louis River water[f]	33 ± 3	390 ± 20	12
Manganika Lake water[g]	19.0 ± 0.6	280 ± 20	14

[a] 10 mg L^{-1} PLFA isolate with no additional thiol species, pH 7

[b] 10 mg L^{-1} PLFA isolate with 10 μM MAA, pH 7

[c] 10 mg L^{-1} PLFA isolate with 10 μM GSH, pH 7

[d] 10 μM MAA with no DOM, pH 7

[e] 10 μM GSH with no DOM, pH 7

[f] filtered Saint Louis River whole water, measured DOC concentration of 25 mg L^{-1}, pH 7.8

[g] 10 mg L^{-1} Manganika Lake isolate with no additional thiol species, pH 7